


## Effects of glycosaminoglycan supplementation in the chondrogenic differentiation of bone marrow- and synovial- derived mesenchymal stem/stromal cells on 3D-extruded poly ( $\epsilon$ -caprolactone) scaffolds

João C. Silva, Carla S. Moura, Gonçalo Borrecho, António P. Alves de Matos, Joaquim M. S. Cabral, Robert J. Linhardt & Frederico Castelo Ferreira


**To cite this article:** João C. Silva, Carla S. Moura, Gonçalo Borrecho, António P. Alves de Matos, Joaquim M. S. Cabral, Robert J. Linhardt & Frederico Castelo Ferreira (2021) Effects of glycosaminoglycan supplementation in the chondrogenic differentiation of bone marrow- and synovial- derived mesenchymal stem/stromal cells on 3D-extruded poly ( $\epsilon$ -caprolactone) scaffolds, *International Journal of Polymeric Materials and Polymeric Biomaterials*, 70:3, 207-222, DOI: [10.1080/00914037.2019.1706511](https://doi.org/10.1080/00914037.2019.1706511)



**To link to this article:** <https://doi.org/10.1080/00914037.2019.1706511>

 View supplementary material 


 Published online: 02 Jan 2020.

 Submit your article to this journal 

 Article views: 230

 View related articles 

 View Crossmark data 

 Citing articles: 3 View citing articles 



## Effects of glycosaminoglycan supplementation in the chondrogenic differentiation of bone marrow- and synovial- derived mesenchymal stem/stromal cells on 3D-extruded poly ( $\epsilon$ -caprolactone) scaffolds

João C. Silva<sup>a,b</sup>, Carla S. Moura<sup>c</sup>, Gonçalo Borrecho<sup>d</sup>, António P. Alves de Matos<sup>d</sup>, Joaquim M. S. Cabral<sup>a</sup>, Robert J. Linhardt<sup>b</sup>, and Frederico Castelo Ferreira<sup>a</sup>

<sup>a</sup>Department of Bioengineering and iBB, Institute for Bioengineering and Biosciences, Instituto Superior Técnico, Universidade de Lisboa, Lisboa, Portugal; <sup>b</sup>Department of Chemistry and Chemical Biology, Biological Sciences, Biomedical Engineering and Chemical and Biological Engineering, Center for Biotechnology and Interdisciplinary Studies, Rensselaer Polytechnic Institute, Troy, NY, USA; <sup>c</sup>CDRSP – Centre for Rapid and Sustainable Product Development, Polytechnic Institute of Leiria, Rua de Portugal-Zona Industrial, Marinha Grande, Portugal; <sup>d</sup>Centro de Investigação Interdisciplinar Egas Moniz (CiEIM), Quinta da Granja, Caparica, Portugal

### ABSTRACT

The lack of effective and long-term treatments for articular cartilage defects has increased the interest for innovative tissue engineering strategies. Such approaches, combining cells, biomaterial matrices and external biochemical/physical cues, hold promise for generating fully functional cartilage tissue. Herein, this study aims at exploring the use of the major cartilage glycosaminoglycans (GAGs), chondroitin sulfate (CS) and hyaluronic acid (HA), as external biochemical cues to promote the chondrogenic differentiation of human bone marrow- and synovium-derived mesenchymal stem/stromal cells (hBMSC/hSMSC) on custom-made 3D porous poly ( $\epsilon$ -caprolactone) (PCL) scaffolds. The culture conditions, namely the chondrogenic medium and hypoxic environment (5% O<sub>2</sub> tension), were firstly optimized by culturing hBMSCs on PCL scaffolds without GAG supplementation. For both MSC sources, GAG supplemented media, particularly with HA, promoted significantly cartilage-like extracellular matrix (ECM) production (higher sulfated GAG amounts) and chondrogenic gene expression. Remarkably, in contrast to tissues generated using hBMSCs, the hSMSC-based constructs showed decreased expression of hypertrophic marker *COL X*. Histological, immunohistochemical and transmission electron microscopy (TEM) analysis confirmed the presence of typical articular cartilage ECM components (GAGs, aggrecan, collagen fibers) in all the tissue constructs produced. Overall, our results highlight the potential of integrating GAG supplementation, hSMSCs and customizable 3D scaffolds toward the fabrication of bioengineered cartilage tissue substitutes with reduced hypertrophy.

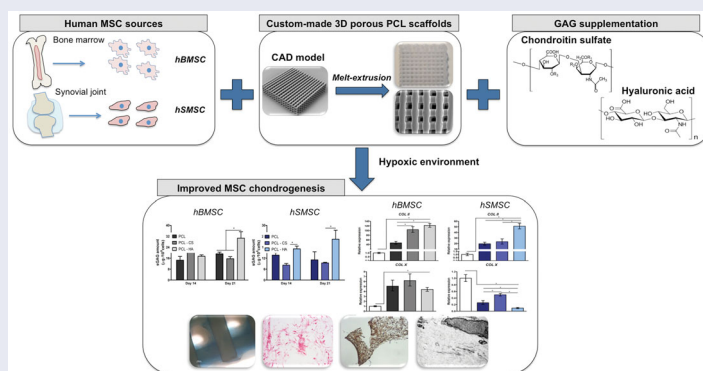
### ARTICLE HISTORY

Received 25 August 2019  
Accepted 5 December 2019

### KEYWORDS

Articular cartilage;  
chondroitin sulfate;  
hyaluronic acid;  
mesenchymal stem/stromal cells; poly ( $\epsilon$ -caprolactone) scaffolds


### GRAPHICAL ABSTRACT



**CONTACT** Frederico Castelo Ferreira ✉ [frederico.ferreira@tecnico.ulisboa.pt](mailto:frederico.ferreira@tecnico.ulisboa.pt) Department of Bioengineering and iBB, Institute for Bioengineering and Biosciences, Instituto Superior Técnico, Universidade de Lisboa, Av. Rovisco Pais, Lisboa 1049-001, Portugal.

Color versions of one or more of the figures in the article can be found online at [www.tandfonline.com/gpom](http://www.tandfonline.com/gpom).

Manuscript prepared and revised for *International Journal of Polymeric Materials and Polymeric Biomaterials*, November 2019.

 Supplemental data for this article can be accessed on the [publisher's website](#).

## 1. Introduction

Articular cartilage is a thin specialized tissue that covers the bone surfaces of synovial joints, enabling mobility with reduced friction and mechanical load dissipation. Due to its avascular constitution and low cellularity, articular cartilage has a limited self-healing capacity on injury upon physical trauma or in degenerative diseases such as osteoarthritis. Osteoarthritis is a progressive chronic joint disease and the leading cause of pain and disability in adults worldwide, comprising nearly \$100 billion of annual healthcare and socioeconomic costs in US<sup>[1,2]</sup>. The growing relevance of joint diseases together with the inability of traditional surgical treatments in generating tissue with native-like features and functionality has resulted in increased interest for innovative cartilage tissue engineering (CTE) strategies. The success of such CTE strategies rely on a proper combination of cells capable of undergoing chondrogenic differentiation upon induction with adequate biochemical/physical factors and biomaterial scaffolds providing a favorable environment for cell growth and cartilage-specific ECM production<sup>[2]</sup>.

Mesenchymal stem/stromal cells (MSC) have been widely explored in CTE as an alternative cell source to chondrocytes mainly due to their easier accessibility, higher proliferative capacity, and advantageous immunomodulatory/trophic properties<sup>[2,3]</sup>. MSCs can be obtained from a wide variety of tissues including bone marrow, adipose tissue, periosteum, muscle, umbilical cord matrix and synovium, however, chondrogenic differentiation potential has been described to be cell source dependent<sup>[4-6]</sup>. Bone marrow-derived MSC (BMSCs) are the most used source and are considered the gold-standard cells for cell-based therapeutic strategies. However, several CTE studies have suggested that synovium-derived MSC (SMSCs) are a superior cell source for cartilage repair due to their higher chondrogenic potential compared to MSCs derived from non-joint tissues<sup>[5-10]</sup>.

Additive manufacturing technologies, such as 3D extrusion, have been widely employed in CTE, exploring their capacity to fabricate scaffolds with the shape and geometry that perfectly match patient's cartilage defect in a fast and reproducible manner<sup>[11,12]</sup>. Synthetic biodegradable polymer poly ( $\epsilon$ -caprolactone) (PCL), previously approved by the US FDA for clinical use, has been used to produce extruded scaffolds in different MSC-based CTE strategies due to its advantageous mechanical, chemical and thermal properties and its ease of processing<sup>[13-15]</sup>.

MSC chondrogenic potential can be enhanced through exposure to specific biochemical (e.g., growth and differentiation modulators such as transforming growth factor- $\beta$ ), physical (e.g., mechanical stimulation) and environmental cues (e.g., oxygen tension)<sup>[16]</sup>. Considering the hypoxic (compared to atmospheric air) nature of articular cartilage *in vivo*, which varies from 1% O<sub>2</sub> tension in the deep zone to 6% O<sub>2</sub> in the superficial zone, as well as of synovial fluid (6.5–9% O<sub>2</sub>) and most MSC niches *in vivo* (1–5% O<sub>2</sub>), different CTE approaches have exploited the use of low oxygen tensions to promote MSC chondrogenesis<sup>[17-19]</sup>. Our group and others previously reported higher *in vitro* proliferative and chondrogenic potential of both BMSCs and SMSCs

when cultured under hypoxic conditions<sup>[20-24]</sup>. A different study also showed augmented chondrogenic differentiation when BMSCs were cultured on porous collagen/hyaluronic acid scaffolds exposed to low oxygen tensions<sup>[25]</sup>.

Glycosaminoglycans (GAGs) are linear, anionic polysaccharides consisting of repeating disaccharide units and either exists as constituents of ECM or on the cell surface covalently attached to core proteins, turning into proteoglycans. Aggrecan is the most predominant proteoglycan in cartilage ECM and consists in a core protein with many GAG chains mainly composed of chondroitin sulfate (CS)<sup>[26,27]</sup>. The highly negatively charged sulfate groups of CS generate electrostatic repulsion and high water uptake, which is crucial for cartilage resistance to compressive forces and shock-absorbing capacity<sup>[28]</sup>. Although present at lower concentrations than CS, hyaluronic acid (HA), which is a non-sulfated GAG, plays a pivotal role in regulating cartilage ECM structural organization and signaling<sup>[28,29]</sup>. Additionally, both CS and HA are known to participate in several signaling pathways, regulating cellular processes such as cell adhesion, migration, proliferation and differentiation through interaction with a wide variety of GAG-binding proteins within the ECM<sup>[26,29]</sup>. Thus, due to their properties and as major components of cartilage, CS and HA have been widely used as CTE scaffolds or hydrogels aiming to improve MSC chondrogenic differentiation<sup>[25,30-32]</sup>. In contrast, the use of GAGs CS and HA as culture medium additives in integrated CTE approaches is much less explored. In fact, few studies have reported the use of GAG supplemented media to promote MSC chondrogenic differentiation in CTE scaffolds, and to the best of our knowledge, none has been conducted using SMSCs or comparing different MSC sources.

The primary aim of the present study was to assess the effects of CS and HA supplementation in the chondrogenic differentiation of MSC on 3D-extruded PCL scaffolds. We hypothesize that integrating predominant cartilage GAGs (CS and HA) as culture medium additives in our CTE strategy might enhance MSC chondrogenic differentiation through a more closely resemble of native tissue's biochemical microenvironment and ECM-cell signaling. Porous PCL scaffolds capable of being tailored to meet patient cartilage defect specificities were fabricated by melt-extrusion and their structural features were characterized. Upon optimization of culturing conditions, two different human MSC sources (hBMSCs and hSMSCs) were studied and their responses to GAG supplementation were compared, by assessing cellularity and cartilage ECM production throughout culture. The quality of the final tissue-engineered cartilage constructs, generated by each MSC source under the different GAG supplementations, was assessed by RT-qPCR, histological/immunohistochemical and transmission electron microscopy (TEM) analysis.

## 2. Materials and methods

### 2.1. Materials

PCL (CAPA<sup>TM</sup> 6500, MW 50000 Da) was obtained from Perstorp Caprolactones, UK. Chondroitin sulfate (CS)

sodium salt from bovine cartilage (REF #C6737) and high-molecular weight hyaluronic acid (HA) sodium salt (REF #53747, MW  $\sim 1.5\text{--}1.8 \times 10^6$  Da) were purchased from Sigma-Aldrich, UK.

## 2.2. Isolation and culture of human MSCs from bone marrow and synovium aspirates

hBMSCs and hSMSCs were isolated and characterized in terms of their immunophenotype and multilineage differentiation potential following protocols previously developed by our group (Supplementary Table 1 and Supplementary Figure 1)<sup>[21,33]</sup>. Bone marrow aspirates were obtained from healthy donors (males with age of 35–36 years) after informed consent, with the approval of the ethics committee of Instituto Português de Oncologia Francisco Gentil. Synovium aspirates were obtained from patients (males with ages between 22 and 28 years) undergoing arthroscopy who had no history of joint disease, after their informed consent at Centro Hospitalar de Lisboa Ocidental, E.P.E., Hospital São Francisco Xavier, Lisboa, Portugal. Isolated hBMSCs and hSMSCs were cultured with Dulbecco's Modified Eagle's Medium (DMEM, Gibco) supplemented with 10% fetal bovine serum (FBS, MSC qualified, Life Technologies) and 1% antibiotic-antimycotic (Anti-Anti, Gibco), and cryopreserved in liquid/vapor-phase nitrogen tanks. All cultures were kept at 37 °C/5% CO<sub>2</sub> in a humidified atmosphere and only cells between passages P3–P6 were used in the experimental assays.

## 2.3. Fabrication and structural characterization of PCL scaffolds

PCL scaffolds were fabricated in a layer-by-layer manner using an in-house developed melt-extrusion machine, the Bioextruder, as previously described<sup>[34,35]</sup>. Briefly, 3D CAD models were designed in SolidWorks software (Dassault Systèmes, S.A.) and the scaffolds were extruded with a 0–90° lay-down fiber orientation with the desired size (dimensions: 7 mm × 7 mm × 3 mm), structure and architecture. In the process, the PCL filament was heated at 80 °C (above PCL's melting temperature  $\sim 60$  °C) and extruded in a built plate through a robot-guided nozzle with motion controlled by a computer. Scaffolds were fabricated using the following extrusion parameters: deposition velocity of 8 mm/sec; rotation velocity of 22.5 rpm; slice thickness of 280  $\mu\text{m}$  and a nozzle diameter of 300  $\mu\text{m}$ , which corresponds to the diameter of a single fiber of the scaffold. The structure of the generated scaffolds was characterized using scanning electron microscopy (SEM, Hitachi S-2400, Japan) and micro-computed tomography ( $\mu$ -CT, Scansky 1174v2, Bruker version 1.1, MA USA).

## 2.4. Optimization of MSC culture conditions on PCL scaffolds: culture medium and oxygen tension

Previous to GAG supplementation *in vitro* cell culture assays, an experiment comparing two different commercially available culture mediums for MSC chondrogenic

differentiation (Hyclone™ AdvanceSTEM™ Chondrogenic Differentiation medium (Hyclone Chondro, Thermo Fisher Scientific, Rockford, IL USA) + 1% Anti-Anti vs. StemPro™ Chondrogenesis Differentiation kit (StemPro Chondro, Gibco™, Thermo Fisher Scientific) + 1% Anti-Anti, with standard expansion medium DMEM + 10% FBS + 1% Anti-Anti used as control) was performed at normoxia conditions. Afterwards, the culture medium with the best performance was used in an additional experiment comparing the effects of three different oxygen tensions (Normoxia: 21% O<sub>2</sub> vs. Hypoxia: 2% O<sub>2</sub> and 5% O<sub>2</sub>) in the chondrogenic differentiation of MSC on PCL scaffolds. The effect of the different oxygen tensions in the proliferative potential of hBMSC in PCL scaffolds was also assessed under standard expansion culture medium (DMEM + 10% FBS).

Before cell seeding, PCL scaffolds were sterilized by UV exposure (2 h each side of the scaffold) and through washing with 70% ethanol for 3 h. Afterwards, the scaffolds were rinsed three times with a phosphate buffered saline (PBS, Gibco) + 1% Anti-Anti solution and moistened with culture medium for 1 h. To perform the optimization experiments,  $1 \times 10^5$  hBMSCs were seeded in each scaffold and incubated without culture medium for 1.5 h to promote initial cell adhesion. Afterwards, the scaffolds were cultured for 21 days under the different culture mediums or oxygen tensions at 37 °C and 5% CO<sub>2</sub>. The culture medium was fully replaced twice a week. The selection of the culture medium and oxygen tension that resulted in the highest hBMSC chondrogenic potential on PCL scaffolds was performed based on the equivalent cell numbers and GAG amounts evaluated as specified in following subsections 2.6 and 2.7, respectively.

## 2.5. hBMSCs and hSMSCs seeding on PCL scaffolds and culture under different GAG supplementation conditions

hBMSCs or hSMSCs were seeded on PCL scaffolds at a density of  $1 \times 10^5$  cells/scaffold and incubated for 1.5 h at 37 °C/5%CO<sub>2</sub> in the absence of culture medium to favor initial cell attachment. Then, Hyclone™ AdvanceSTEM™ Chondrogenic Differentiation medium + 1% Anti-Anti supplemented with different predominant cartilage GAGs (CS and HA) was added to the scaffolds. For that, based on previously reported values of GAG concentration in healthy human knee and synovial joint fluid, sterile CS and HA were dissolved in culture medium to generate 2% CS and 0.4% HA (w/v) medium supplemented solutions<sup>[36–38]</sup>. Thus, three different experimental groups were considered for each cell source according to the GAG-supplemented medium used: (i) non-supplemented control (PCL), (ii) CS-supplemented (PCL-CS) and (iii) HA-supplemented (PCL-HA). All cultures were maintained in a hypoxic environment (5% O<sub>2</sub> tension) to provide a closer mimic of the native articular cartilage niche and promote MSC chondrogenesis. The experiment was conducted for 21 days and culture medium was fully renewed twice a week.



**Table 1.** Primer sequences used in this study for RT-qPCR analysis.

Gene	Forward primer sequence	Reverse primer sequence
<i>GAPDH</i>	5'-GGTCACCAGGCTGCTTTTA-3'	5'-CTGGAAGATGGTGATGGGA-3'
<i>COL I</i>	5'-CATCTCCCTTCGTTTTGA-3'	5'-CCAAATCCGATGTTTCTGCT-3'
<i>COL II</i>	5'-GGAATTCCTGGAGCCAAAGG-3'	5'-AGGACCAGTCTTGAG-3'
<i>ACAN</i>	5'-CACTGGCGAGCACTGAACAT-3'	5'-TCCACTGGTAGTCTTGGGCAT-3'
<i>COL X</i>	5'-CCAGGTCTGGATGGTCTTA-3'	5'-GTCCTCAAACCTCCAGGATCA-3'
<i>Runx2</i>	5'-AGATGATGACACTGCCACCTCTG-3'	5'-GGGATGAAATGCTTGGGAAC-3'

## 2.6. Cell proliferation assay

The metabolic activity of hBMSCs/hSMSCs in the different GAG supplementation experimental groups was evaluated throughout the culture period (days 1, 7, 14, and 21) using AlamarBlue<sup>®</sup> cell viability reagent (ThermoFischer Scientific, USA) following the manufacturer's guidelines. Briefly, a 10% (v/v) AlamarBlue<sup>®</sup> solution in culture medium was added to the scaffolds and incubated at 37 °C in 5% CO<sub>2</sub> chamber for 2.5 h. Fluorescence intensity was measured in a plate reader (Infinite<sup>®</sup> M200 PRO, TECAN, Switzerland) at an excitation/emission wavelength of 560/590 nm and compared to a calibration curve (specific for each donor and culture medium used) to access the equivalent number of cells in each scaffold. Acellular scaffolds (for each experimental group) were used as blank controls in the fluorescence intensity measurements. In each experiment, three different scaffolds were considered for each experimental group and fluorescence intensity values of each sample were measured in triplicate.

## 2.7. Alcian blue staining and sGAG quantification assay

At days 14 and 21 of the differentiation protocol, scaffold samples were harvested, washed thoroughly with PBS to remove all medium remnants, and fixed with 2% w/v paraformaldehyde (PFA, Sigma-Aldrich) solution for 20 min. Afterwards, samples were washed with PBS and incubated with 1% w/v Alcian Blue 8GX (Sigma-Aldrich) solution (in 0.1 N hydrochloric acid, Sigma-Aldrich) for 1 h to assess for the presence of sulfated GAG (sGAG). The samples were rinsed twice with PBS, washed once with distilled water and imaged using a LEICA<sup>®</sup> DMI3000B (Leica Microsystems, Germany) microscope equipped with a digital camera (Nikon DXM1200F, Nikon Instruments Inc., Japan). sGAG content in the scaffolds of the different experimental groups was quantified by Alcian Blue dye precipitation following previously reported protocols<sup>[39,40]</sup>. For that, Alcian Blue stained samples were treated with a 2% w/v sodium dodecyl sulfate (SDS, Sigma-Aldrich) solution with constant shaking overnight. The absorbance of the resultant solutions was measured in a plate reader (Infinite<sup>®</sup> M200 PRO, TECAN) at 620 nm, compared to a calibration curve to estimate the sGAG content and normalized to the equivalent number of cells present in each scaffold. For each independent experiment, three scaffolds were considered for each condition and the absorbance of each sample was measured in triplicate.

## 2.8. RNA isolation and gene expression analysis by real time quantitative PCR

At day 21, scaffolds cultured with hBMSCs and hSMSCs under the different GAG stimulation conditions were collected for gene expression analysis by real time quantitative PCR (RT-qPCR). Total RNA was extracted using the RNeasy Mini Kit (QIAGEN, Hilden, Germany) according to the manufacturer's protocol and quantified by UV spectrophotometry using a Nanodrop (NanoVue Plus, GE Healthcare, Chicago, IL USA). cDNA was synthesized from the isolated RNA using iScript<sup>™</sup> Reverse Transcription Supermix (Bio-Rad, Hercules, CA USA) according to manufacturer's guidelines. Reaction mixtures (20 µl) were incubated in a T100<sup>™</sup> thermal cycler (Bio-Rad) with the following temperature protocol: 5 min at 25 °C, 20 min at 46 °C and 1 min at 95 °C. RT-qPCR was performed using Fast SYBR<sup>™</sup> Green Master Mix (Applied Biosystems, CA USA) and the StepOnePlus real-time PCR equipment (Applied Biosystems). All reaction mixtures (20 µl) containing the specific primer sequences for the target genes and cDNA template were carried out in accordance with the manufacturer's guidelines and using the following temperature protocol: denaturation step at 95 °C for 20 sec, followed by 40 cycles of 95 °C for 3 sec and 60 °C for 30 sec. All samples were assayed in triplicate and the results were analyzed using the 2<sup>-ΔΔCt</sup> method. Target genes (collagen type I (*COL I*), collagen type II (*COL II*), Aggrecan (*ACAN*), collagen type X (*COL X*) and runt-related transcription factor 2 (*Runx2*)) expression was primarily normalized to the house-keeping gene glyceraldehyde 3-phosphate dehydrogenase (*GAPDH*) and then determined as a fold-change relative to the baseline expression of hBMSCs or hSMSCs at day 0. The specific primer sequences used in the RT-qPCR analysis are presented in Table 1.

## 2.9. Histological/immunohistochemical analysis

The final hBMSCs/hSMSCs-PCL constructs generated under different GAG stimulations were fixed in 4% PFA and embedded in Bio-Agar (Bio-Optica, Italy). Afterwards, the samples were dehydrated with progressive graded ethanol series (70%, 95%, 100%), cleared with xylene and embedded in paraffin. The paraffin blocks were sliced into 5 µm sections using a microtome Leica RM2235 (Leica Biosystems) and mounted in glass slides. Afterwards, upon deparaffinization and rehydration of the slides, endogenous peroxidase activity was blocked with 3% hydrogen peroxidase treatment (H<sub>2</sub>O<sub>2</sub>, Sigma-Aldrich) for 10 min. For histological assessment of the constructs, slides were stained with hematoxylin-eosin (H&E, Sigma-Aldrich) for 5 min to visualize cells/cell nuclei, Toluidine Blue (0.1% w/v aqueous solution, Sigma-Aldrich) for 5 min to identify proteoglycans and with Safranin-O (1% w/v aqueous solution, Sigma-Aldrich) for 15 min to observe secreted GAG. Regarding the immunohistochemical analysis, sections were incubated overnight at room temperature with rabbit polyclonal antibodies to collagen II (1:800 dilution, Anti-Collagen II antibody ab34712, Abcam, UK) and aggrecan (1:250 dilution, Anti-Aggrecan II

antibody ab140707, Abcam, UK); and visualized after incubation for 30 min with anti-rabbit Dako EnVision<sup>+</sup> System-HRP Labeled Polymer (Agilent Dako, CA USA). The slides were finally counterstained with hematoxylin, dehydrated and mounted. The images of histological and immunohistological analysis were obtained at 200 $\times$  magnification using a Leica DMLB optical microscope equipped with a DFC290 HD camera (Leica Microsystems).

### 2.10. Transmission electron microscopy (TEM) analysis

At the end of the experiment, culture medium was removed; samples were washed with PBS and fixed with a 3% (v/v) glutaraldehyde (Sigma-Aldrich) in 0.1 M sodium cacodylate buffer (Sigma-Aldrich) solution overnight at 4 $^{\circ}$ C. Samples were kept in 0.1 M sodium cacodylate buffer at 4 $^{\circ}$ C until further processing. The fixed samples were embedded in agar, rinsed with cacodylate buffer and post-fixed with a 1% (v/v) osmium tetroxide (Sigma-Aldrich) solution in 0.1 M cacodylate buffer for 1 h at room temperature. Afterwards, the constructs were fixed with 1% uranyl acetate (Sigma-Aldrich) in acetate acetic acid buffer 0.1 M (v/v, pH 5.0) for 1 h and dehydrated by exposure to gradually increasing ethanol concentrations (70%, 95% and 100% in distilled water; 3  $\times$  10 min each). Additionally, the constructs were treated twice with propylene oxide (Sigma-Aldrich) for 15 min, incubated with epoxypropane for 1 h and embedded in epoxy resin (Epon<sup>TM</sup>, Hexion Inc., Columbus, OH USA). Finally, samples were cut with a diamond knife (0.5  $\mu$ m slices) in a Reichert Ultracut E ultramicrotome (Leica Microsystems) and the ultrastructure of cells and ECM of the different constructs was imaged using a JEOL 1200EX TEM equipment (JEOL USA, Inc., MA USA).

### 2.11. Statistical analysis

Results are presented as mean values  $\pm$  standard error of mean (SEM). Each experiment was conducted using at least three biological replicates ( $n = 3$ ), unless otherwise specified. Statistical analysis of the data was performed using one-way ANOVA, followed by Tukey post-hoc test. GraphPad Prism version 7 software was used in the analysis and data was considered to be significant when  $p$ -values obtained were less than 0.05 (95% confidence intervals) ( $*p < 0.05$ ).

## 3. Results

### 3.1. Fabrication and characterization of 3 D-extruded porous PCL scaffolds

Custom-made porous PCL scaffolds with a 0–90 $^{\circ}$  fiber orientation pattern and a pore size of 390  $\mu$ m (Figure 1A) were fabricated using an in-house developed 3 D-extrusion equipment and their structure/morphological properties were assessed by SEM (Figure 1B) and  $\mu$ -CT (Figure 1C) as previously described<sup>[35]</sup>.  $\mu$ -CT analysis of the PCL scaffolds estimated high porosity of approximately 57% and high interconnectivity of 99.7%, which is beneficial for cell infiltration and also favors efficient nutrient supply, gas diffusion and waste removal.

### 3.2. Optimization of MSC culture on PCL scaffolds: chondrogenic culture medium and oxygen tension selection

Before studying the effects of CS and HA supplementation on hBMSC and hSMSC chondrogenic differentiation in PCL scaffolds, preliminary experimental assays were performed

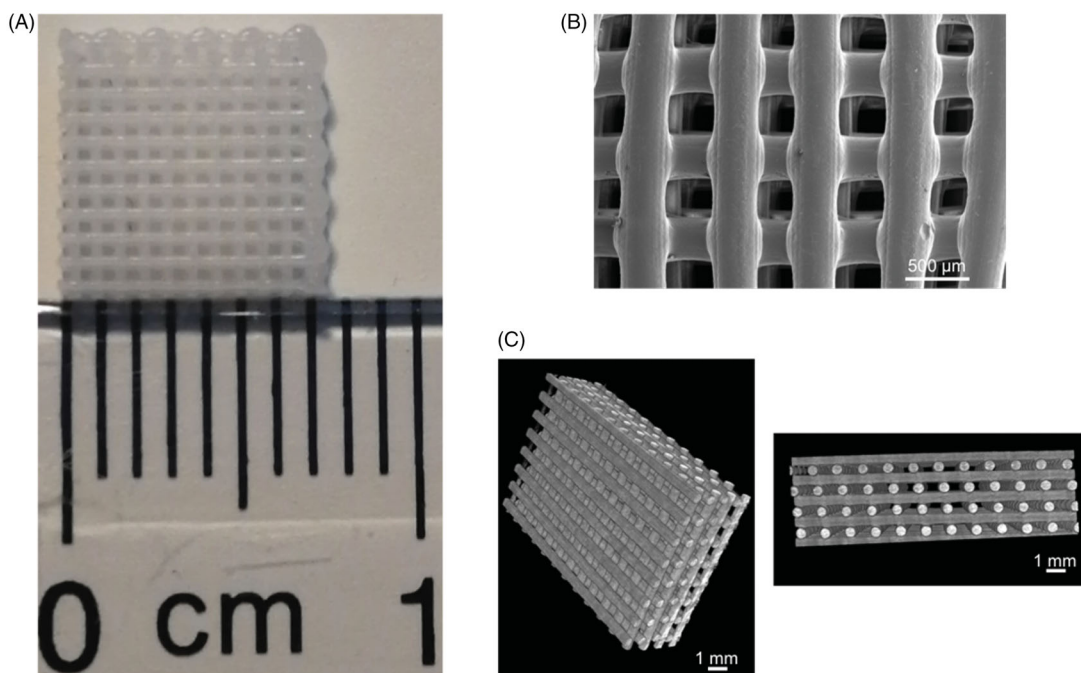


**Figure 1.** Characterization of 3 D-extruded PCL scaffold: macroscopic view (A), SEM micrograph (B) and 3 D reconstruction images obtained after  $\mu$ -CT analysis (C). Scale bars are depicted in the figure.

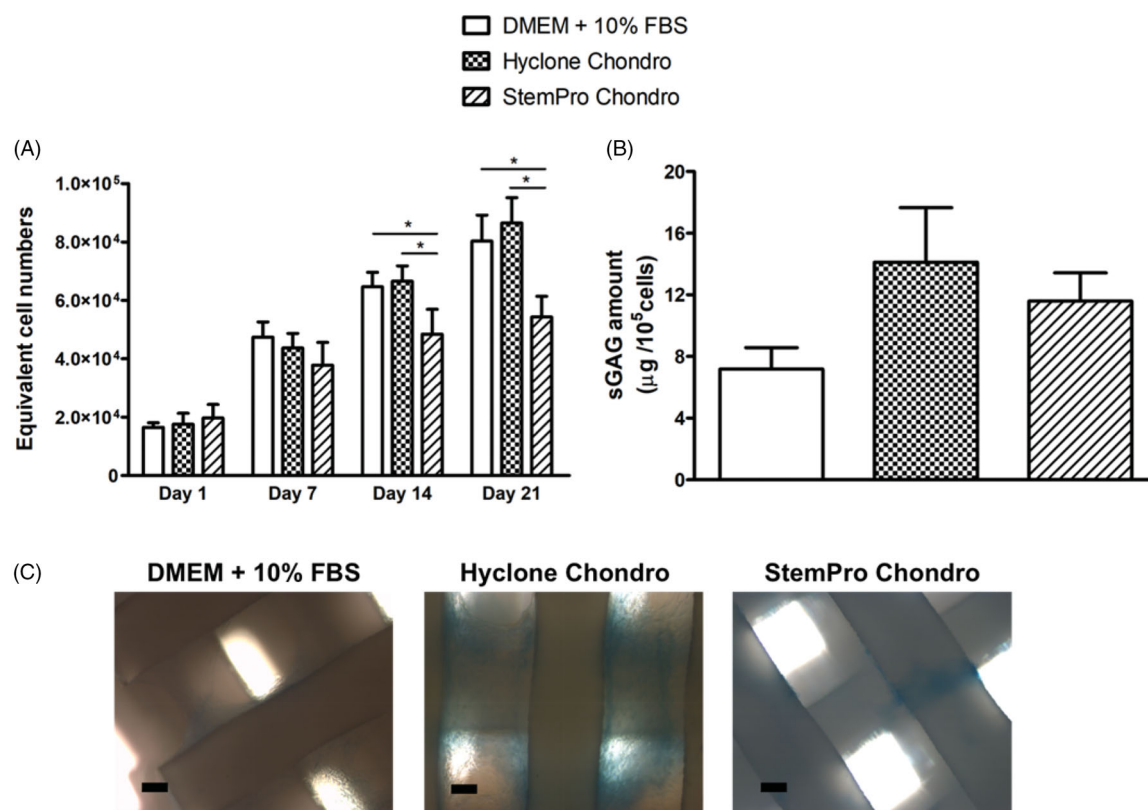


**Figure 2.** Comparison of different commercially available culture medium for the chondrogenic differentiation of hBMSC on PCL scaffolds. Equivalent cell numbers assessed by Alamar Blue assay throughout the culture period (A) and sGAG amount at the end of the experiment (B) for the different culture medium tested. Alcian Blue staining (C) was performed in the final tissue constructs (day 21). Results are presented as average  $\pm$  SEM of three ( $n = 3$ ) independent experiments. \* $p < 0.05$ . Scale bar: 100  $\mu\text{m}$ .

using hBMSC to select the chondrogenic medium (between two commercially available formulations) and oxygen tension (2%  $\text{O}_2$ , 5%  $\text{O}_2$  and 21%  $\text{O}_2$ ) with improved results concerning the equivalent number of cells and sGAG production in the 3D PCL scaffold culture system.

Regarding the chondrogenic medium selection (Figure 2), hBMSC-PCL constructs cultured under Hyclone Chondro medium presented significantly higher ( $p < 0.05$ ) equivalent cells numbers at days 14 and 21 than the ones cultured under StemPro Chondro medium (Figure 2A). As shown in Figure 2B, PCL-hBMSC constructs cultured for 21 days with Hyclone Chondro medium presented sGAG amounts ( $14.1 \pm 3.6 \mu\text{g}/10^5$  cells) higher than the ones cultured in StemPro Chondro ( $11.6 \pm 1.8 \mu\text{g}/10^5$  cells) and control DMEM + 10% FBS ( $7.2 \pm 1.4 \mu\text{g}/10^5$  cells). Alcian Blue staining images (Figure 2C) demonstrate that hBMSC-PCL constructs cultured under both chondrogenic mediums stained positively for GAG deposition, however the staining appeared more predominant and distributed along the scaffold when Hyclone Chondro was used. Although at a lower intensity, it was also possible to observe positive staining when constructs were maintained in standard expansion medium (DMEM + 10% FBS) without addition of any chondroinductive supplements, suggesting that PCL scaffold alone supports some level of GAG secretion by MSCs.

The effect of oxygen tension in the hBMSC proliferation on PCL scaffolds was assessed using expansion medium (DMEM + 10% FBS). Scaffolds cultured under both low

oxygen tensions (2%  $\text{O}_2$  and 5%  $\text{O}_2$ ) showed increased cell proliferation comparing to normoxia condition, presenting significantly ( $p < 0.05$ ) higher cell numbers (Figure 3A) and fold increases (Figure 3B) from day 14 onwards. At day 21, hBMSC scaffold culture under the different oxygen tensions reached equivalent cell numbers and fold increases in cell number (relative to day 1) of  $1.21 \pm 0.04 \times 10^5$  cells and  $5.17 \pm 0.16$  for 2%  $\text{O}_2$ ,  $1.23 \pm 0.08 \times 10^5$  cells and  $4.78 \pm 0.30$  for 5%  $\text{O}_2$  and  $1.02 \pm 0.11 \times 10^5$  cells and  $3.67 \pm 0.39$  for 21%  $\text{O}_2$ . hBMSC chondrogenic differentiation under the three different oxygen tensions was also performed culturing the cell-scaffold constructs with Hyclone Chondro medium. Figure 3C shows that cultures under both hypoxia conditions resulted in significantly ( $p < 0.05$ ) higher equivalent cell numbers (from day 7 onwards) when compared to the ones at 21%  $\text{O}_2$ . At day 21, the hBMSC-PCL constructs cultured under the different oxygen tensions showed GAG deposition upon Alcian Blue staining (Figure 3E) and resulted in sGAG amounts of  $12.3 \pm 0.5 \mu\text{g}/10^5$  cells,  $18.3 \pm 0.9 \mu\text{g}/10^5$  cells ( $p < 0.05$  relative to 2%  $\text{O}_2$ ) and  $16.1 \pm 2.0 \mu\text{g}/10^5$  cells for 2%  $\text{O}_2$ , 5%  $\text{O}_2$  and 21%  $\text{O}_2$ , respectively (Figure 3D).

### 3.3. Effects of CS and HA supplementation on hBMSC/hSMSC chondrogenic differentiation

Based on the results of the previous section, the effects of CS and HA supplementation on the chondrogenic



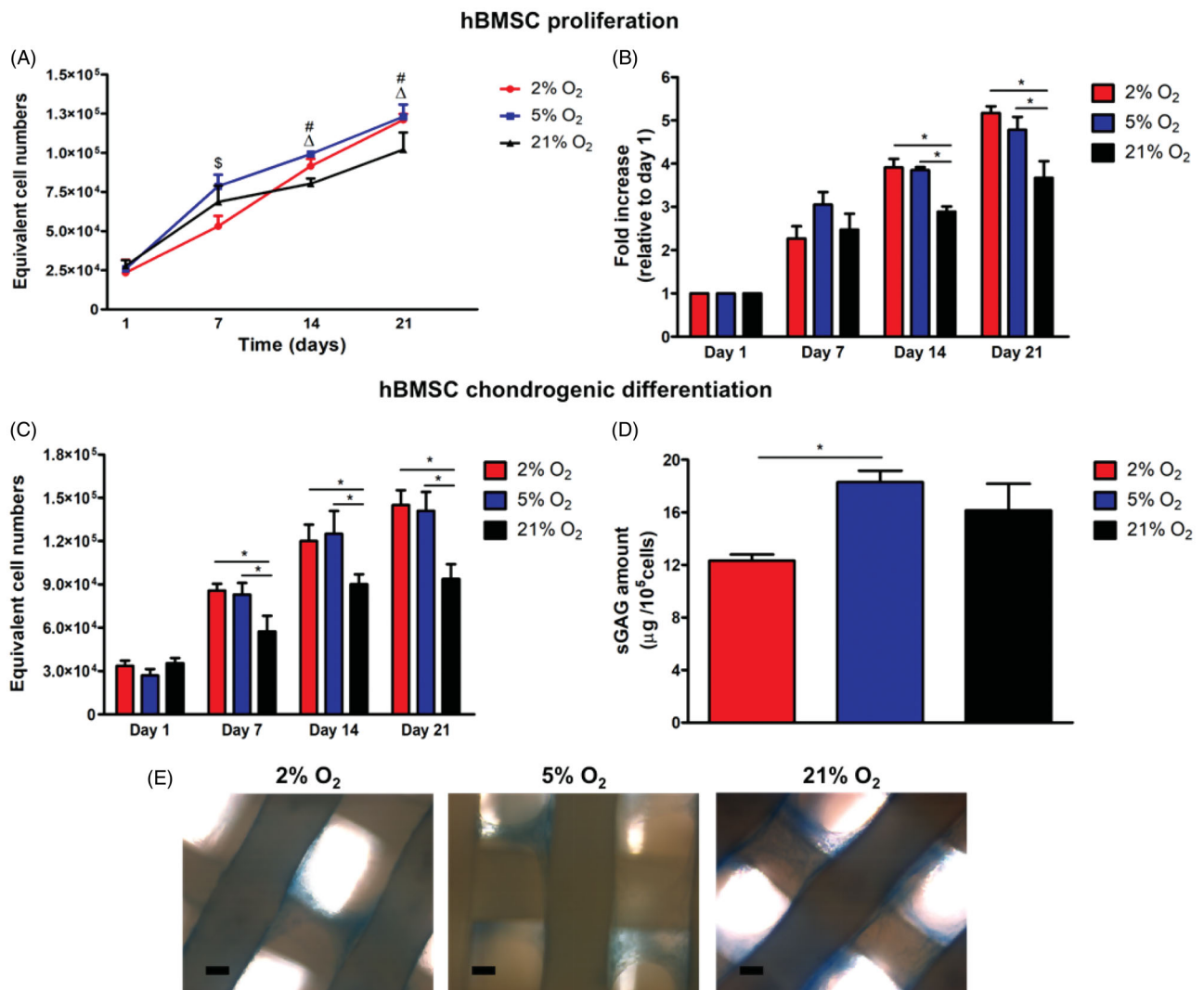


**Figure 3.** Effects of oxygen tension in hBMSC culture on PCL scaffolds. Cell proliferation evaluated by Alamar Blue assay (A) throughout culture (#,  $\Delta$  and  $\$$  correspond to statistical difference between 2%  $O_2$  vs. 21%  $O_2$ , 5%  $O_2$  vs. 21%  $O_2$  and 2%  $O_2$  vs. 5%  $O_2$ , respectively) and fold increase in cell numbers relative to day 1 (B). hBMSC chondrogenic differentiation under different oxygen tensions was evaluated by assessment of equivalent cell numbers throughout culture (C), sGAG amounts (D) and Alcian Blue staining (E) at the end of the experiment day 21. Results are presented as average  $\pm$  SEM of three ( $n=3$ ) independent experiments. \* $p < 0.05$ . Scale bar: 100  $\mu\text{m}$ .

differentiation of hBMSC and hSMSC on PCL scaffolds (Figure 4) were studied using Hyclone Chondro medium and 5%  $O_2$  tension. For both hBMSC (Figure 4A) and hSMSC (Figure 4B), GAG supplementation did not show any significant effect on the equivalent cell numbers throughout all the 21 days of culture.

Regarding sGAG amounts in hBMSC-based constructs (Figure 4C), no significant differences were observed among the different conditions at day 14. It was noteworthy that at day 21, the PCL-HA group generated sGAG amounts ( $30.6 \pm 4.7 \mu\text{g}/10^5$  cells) significantly higher ( $p < 0.05$ ) than the PCL-CS ( $15.6 \pm 1.5 \mu\text{g}/10^5$  cells) and PCL ( $19.2 \pm 1.3 \mu\text{g}/10^5$  cells) groups. In the case of hSMSC-based constructs (Figure 4D), HA-supplementation originated constructs with significantly increased ( $p < 0.05$ ) sGAG amounts than the ones cultured under CS-supplementation both at day 14 and 21. After 21 days of chondrogenic differentiation, the amounts of sGAG produced by hSMSC in PCL, PCL-CS and PCL-HA groups were  $11.1 \pm 4.5 \mu\text{g}/10^5$  cells,  $9.4 \pm 0.4 \mu\text{g}/10^5$  cells and  $22.4 \pm 4.9 \mu\text{g}/10^5$  cells, respectively. Figure 4E

shows Alcian Blue staining images (at day 21) of both hBMSC-PCL and hSMSC-PCL constructs cultured under the different GAG-supplemented mediums. All constructs stained positively for Alcian Blue, therefore confirming the presence of secreted GAGs.

### 3.4. Gene expression analysis

The expression of genes associated with chondrogenesis and tissue hypertrophy in the final hBMSC/hSMSC-PCL constructs (day 21) cultured under different GAG supplementation was evaluated by RT-qPCR analysis (Figure 5). Both hBMSC-PCL (Figure 5A) and hSMSC-PCL (Figure 5B) tissue engineered constructs showed a significant downregulation ( $p < 0.05$ ) of fibrocartilage marker *COL I* expression compared to the respective cell source before scaffold seeding (day 0). Regarding the hBMSC-PCL constructs, both CS and HA supplementation resulted in a significantly higher ( $p < 0.05$ ) *COL II* expression when compared with non-



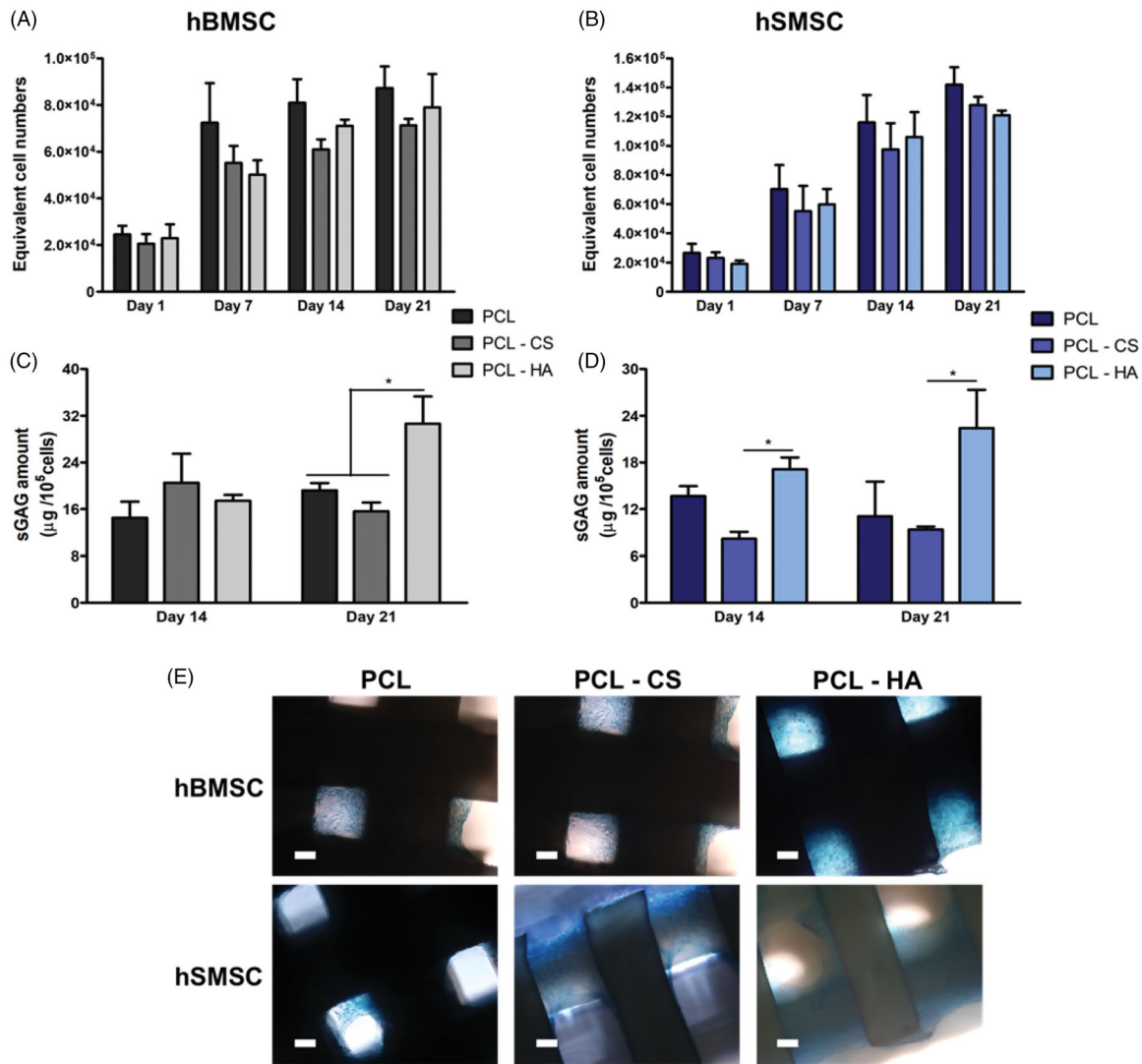


**Figure 4.** Effects of CS and HA supplementation on the chondrogenic differentiation of hBMSC/hSMSC in PCL scaffolds. Equivalent cell numbers estimated using the Alamar Blue assay for hBMSC-PCL (A) and hSMSC-PCL (B) constructs throughout all culture time. sGAG amounts analyzed at day 14 and 21 in hBMSC-PCL (C) and hSMSC-PCL (D) constructs. Alcian Blue staining (E) to identify sulfated GAGs presence in the final tissue constructs (day 21). Results are presented as average  $\pm$  SEM of three ( $n = 3$ ) independent experiments. \* $p < 0.05$ . Scale bar: 100  $\mu$ m.

supplemented PCL group. However, PCL-CS and PCL-HA groups *COL II* expressions were not statistically different ( $p > 0.05$ ) between them (Figure 5C). Interestingly, in the hSMSC-derived constructs, PCL-HA group presented significantly higher ( $p < 0.05$ ) *COL II* expression levels than both PCL and PCL-CS groups, which were not significantly different among them (Figure 5D). Concerning *ACAN* expression, while significant upregulation (relative to hBMSCs at day 0) was observed for all hBMSC-PCL groups, without significant differences among these (Figure 5E), in hSMSC-PCL constructs, only PCL-HA showed increased *ACAN* expression with significantly higher ( $p < 0.05$ ) levels than both PCL and PCL-CS groups (Figure 5F). All hBMSC-PCL constructs presented a significant upregulation of cartilage hypertrophic marker *COL X* (Figure 5G). In contrast, the hSMSC-PCL constructs showed significant *COL X* downregulation compared to hSMSC at day 0, regardless of the GAG-supplementation protocol used. Additionally, the PCL-HA group presented significantly reduced ( $p < 0.05$ ) *COL X*

expressions compared to the other two groups (Figure 5H). Regarding osteogenic marker *Runx2* expression, all hBMSC-PCL (Figure 5I) constructs showed significant upregulation, while for hSMSC-PCL (Figure 5J), only the non-supplemented group presented significantly increased expression levels when compared to the respective MSC source before scaffold seeding (day 0). It was noteworthy that for both MSC sources, HA supplementation resulted in final tissue engineered constructs with significantly decreased ( $p < 0.05$ ) *Runx2* expressions compared to the respective non-supplemented PCL group. Moreover, a similar effect was also observed in hSMSC-PCL constructs when cultured under CS supplementation.

### 3.5. Histological, immunohistochemical and TEM analysis

The final hBMSC-PCL and hSMSC-PCL engineered constructs generated after 21 days of culture under the different

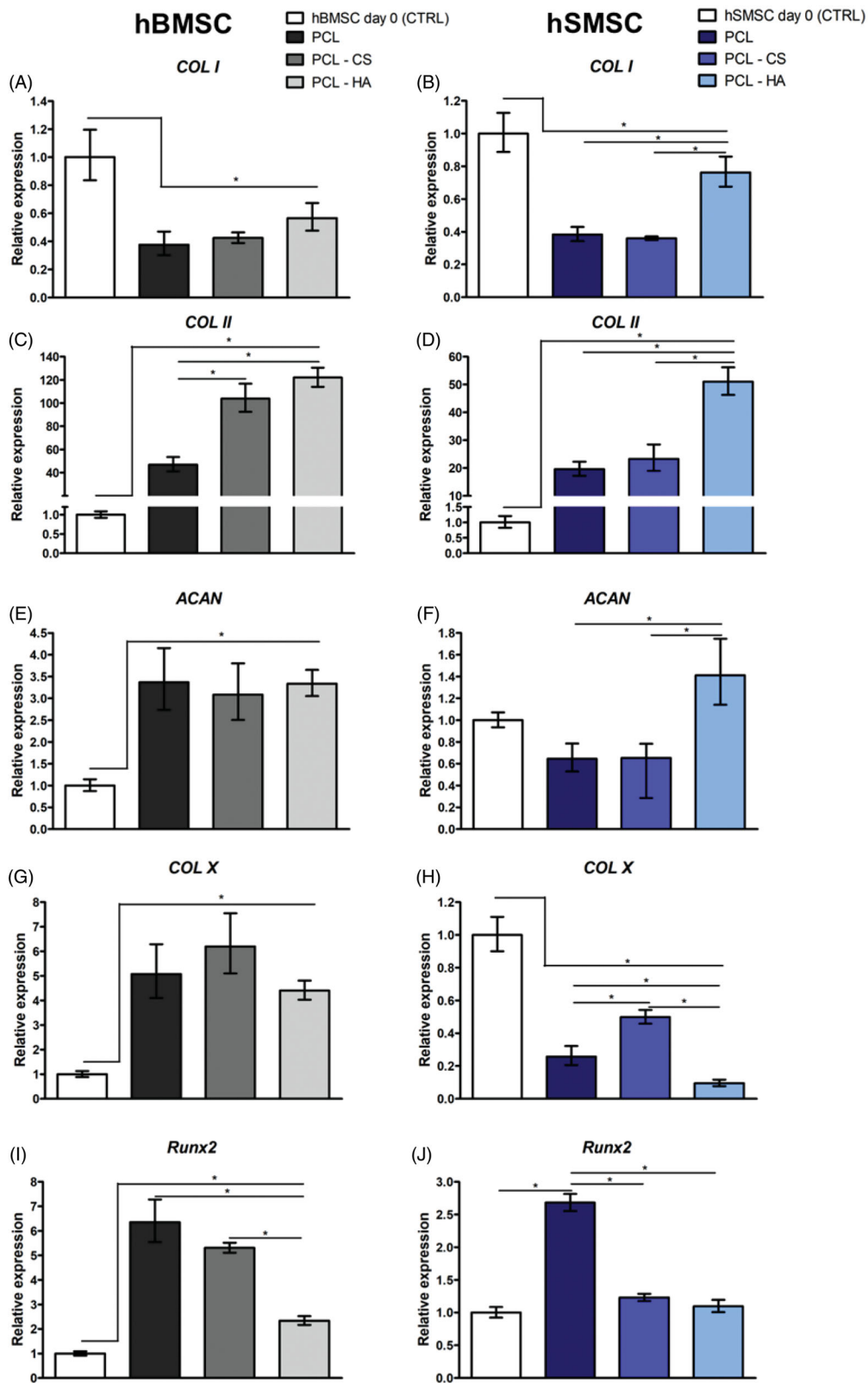


**Figure 5.** RT-qPCR analysis of the final hBMSC/hSMSC-PCL constructs generated under the different GAG supplementations (day 21). *COL I* (A,B), *COL II* (C,D), *ACAN* (E,F), *COL X* (G,H) and *Runx2* (I,J) gene expressions are normalized against the housekeeping gene *GAPDH* and presented as fold-change levels relative to hBMSC/hSMSC at day 0 prior to scaffold seeding. \* $p < 0.05$ .

GAG-supplemented mediums were processed and evaluated by histological (Figure 6), immunohistochemical (Figure 7) and TEM (Figure 8) analysis.

Representative histological images after H&E staining, confirmed the presence and distribution of cells with defined

nuclei in all hBMSC-PCL (Figure 6A) and hSMSC-PCL (Figure 6B) tissue constructs cultured under different GAG supplementations. Additionally, Toluidine Blue and Safranin-O positive staining in all the experimental groups of hBMSC-PCL (Figure 6A) and hSMSC-PCL (Figure 6B)

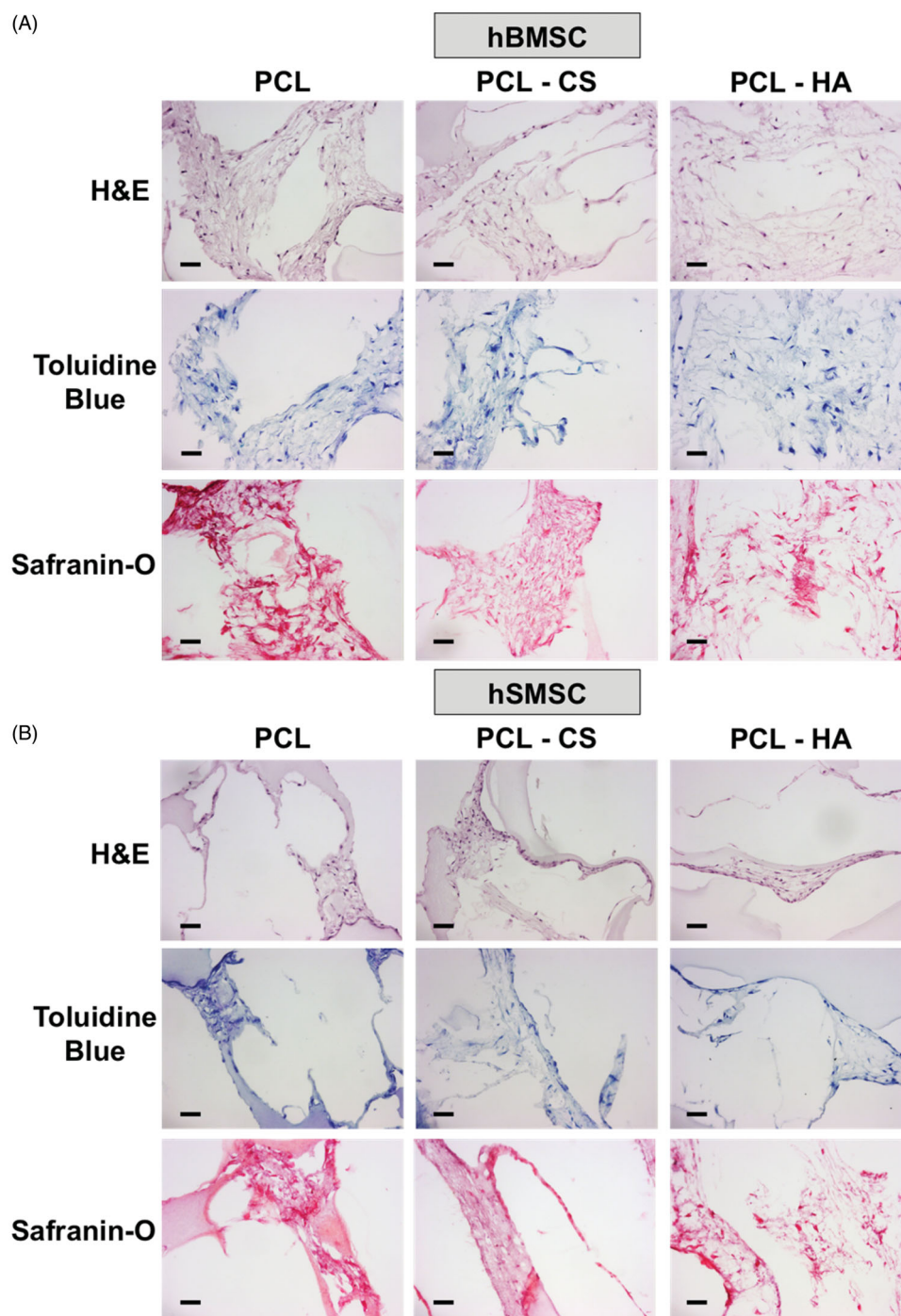


**Figure 6.** Histological analysis of the final hBMSC-PCL (A) and hSMSC-PCL (B) tissue constructs obtained under the different GAG supplementations (day 21). H&E staining to identify cell nuclei, Toluidine Blue staining to assess the presence of proteoglycans and Safranin-O staining for sulfated GAGs identification. Scale bar: 50  $\mu$ m.

engineered tissues confirmed the presence proteoglycans and GAGs, respectively.

Figure 7 shows the representative images resultant from the immunodetection analysis performed on the final hBMSC-PCL (Figure 7A) and hSMSC-PCL (Figure 7B) constructs to assess for the presence of cartilage ECM components, collagen II and aggrecan (brown stain). Collagen II protein expression was clearly observed in all the experimental groups tested, regardless of the GAG supplementation and MSC source. Nevertheless, the immunohistochemical images suggested a more intense and spread

collagen II protein expression in the hBMSC-PCL tissue constructs. All hBMSC-PCL and hSMSC-PCL constructs stained positively for the presence of major cartilage proteoglycan aggrecan. However, for both cell sources, PCL-CS and PCL-HA experimental groups exhibited a more abundant and distributed positive staining for aggrecan presence than PCL.

The ultrastructure of the cells and ECM present in the final hBMSC-PCL/hSMSC-PCL tissue constructs obtained after 21 days of chondrogenic differentiation under different GAG supplementations was analyzed by TEM and can be

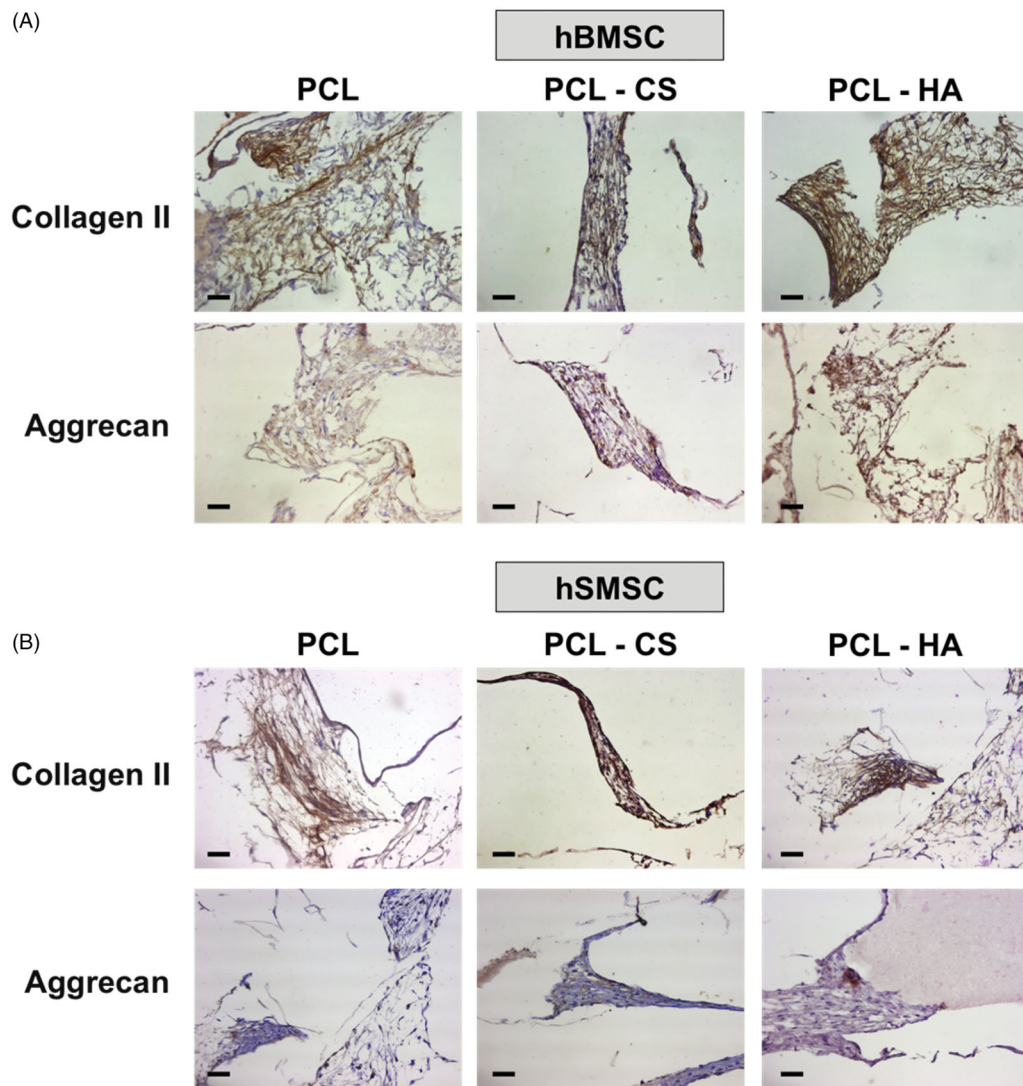


**Figure 7.** Immunohistochemical analysis of the final hBMSC-PCL (A) and hSMSC-PCL (B) tissue constructs obtained under the different GAG supplementations (day 21). Positive staining for collagen II and aggrecan is observed in brown and samples were counterstained with hematoxylin. Scale bar: 50  $\mu\text{m}$ .

observed in Figure 8. TEM images of all experimental groups showed cells embedded in a dense ECM, however the presence of collagen fibers characteristic of cartilage ECM, was more evident, for both MSC sources, when tissue constructs were generated under CS and HA supplementation.

#### 4. Discussion

The objective of this work was to evaluate the effects of CS and HA supplementation as medium additives in the chondrogenic differentiation of MSCs on 3D porous PCL scaffolds. In this study, two different sources of MSC (hBMSC and hSMSC) were considered and their responses to GAG supplementation were compared. These sources were selected due to their reported superior chondrogenic ability in CTE strategies<sup>[4,5]</sup>. As a result of the ease of processing, and its versatility and good mechanical properties, PCL has been widely used in additive manufacturing-based strategies for cartilage repair<sup>[13,41]</sup>. The scaffolds fabricated in this

study presented high porosity and high interconnectivity, and a pore size of 390  $\mu\text{m}$ , which falls within the range of pore sizes (300–450  $\mu\text{m}$ ) previously reported to favor MSC chondrogenic differentiation in 3D PCL scaffolds<sup>[42,43]</sup>.

As gold-standard cells for cellular therapy and most used cell source in CTE strategies, hBMSC were used in the optimization studies to select the culture medium and oxygen tension with highest chondrogenic potential. Hyclone Chondro, the chondrogenic medium that generated higher cell metabolic activities and sGAG production, has also been successfully employed in other CTE approaches using MSC isolated from different sources<sup>[44,45]</sup>. Regarding the oxygen tension study, both 2% and 5%  $\text{O}_2$  hypoxia conditions promoted a significantly higher hBMSC proliferation in PCL scaffolds than the normoxia (21%  $\text{O}_2$ ) condition. Accordingly, different studies have previously reported enhanced proliferation of both hBMSC and hSMSC in 2D tissue culture plates when cultured under hypoxic conditions<sup>[20,21,24]</sup>. Additionally, in accord with our observations, Grayson *et al* showed improved hBMSC proliferation in 3D



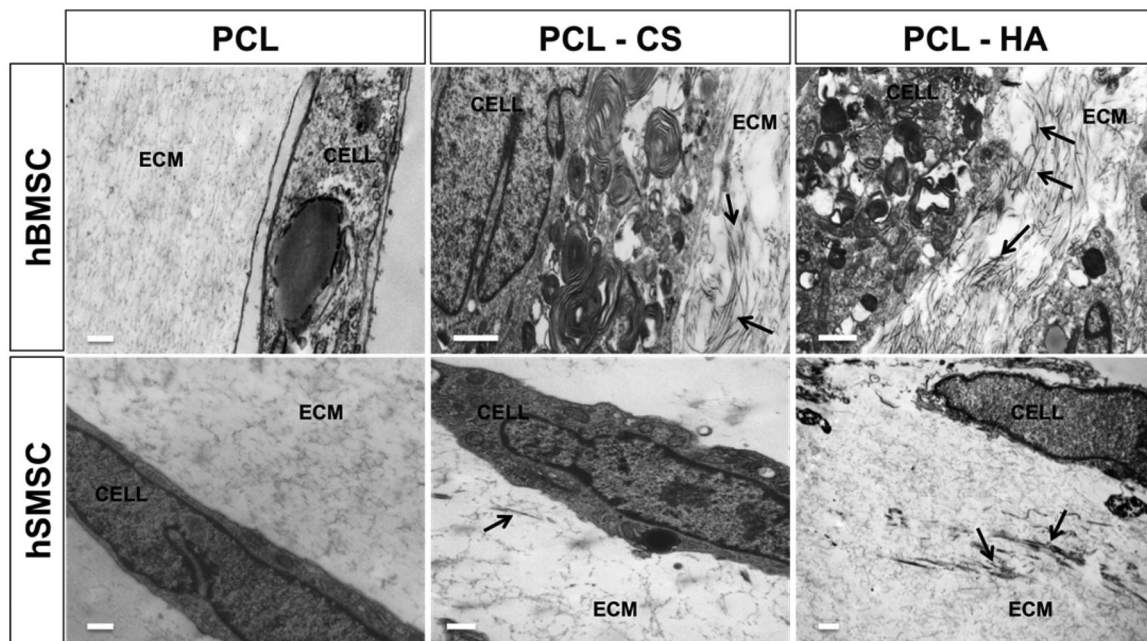


**Figure 8.** TEM images of ECM present in the final hBMSC-PCL and hSMSC-PCL tissue constructs generated under the different GAG supplementations (day 21). Black arrows highlight the presence of collagen fibers. Scale bar: 1  $\mu\text{m}$ .

poly (ethylene terephthalate) scaffolds when exposed to hypoxia (2%  $\text{O}_2$ )<sup>[46]</sup>. In the present study, chondrogenic differentiation of hBMSC in PCL scaffolds under hypoxia (5%  $\text{O}_2$ ) resulted in higher sGAG production than the other oxygen tensions tested. Over the past few years, several studies have reported a positive effect of hypoxic cultures in increasing the sGAG amounts produced by BMSC under chondrogenic induction, either cultured as 3D micromasses/pellets or seeded in 3D biomaterial scaffolds<sup>[22,23,47,48]</sup>. Rodenas-Rochina *et al* reported considerable higher amounts of sGAGs secreted by BMSCs differentiated in PCL scaffolds under hypoxia (5%  $\text{O}_2$ ) than the ones cultured at normoxia (21%  $\text{O}_2$ )<sup>[48]</sup>. Interestingly, we observed a significantly decreased sGAG amount in the constructs cultured under 2%  $\text{O}_2$  compared to the ones at 5%  $\text{O}_2$ . Nevertheless, it is important to note that the oxygen tension values reported are the ones controlled in the incubator, which differ than those experienced by cells that are hard to determine due to technological limitations. Accordingly, Fink *et al.* demonstrated that monolayer cultures of human MSCs showed a considerably lower  $\text{O}_2$  tension at the cell surface than the one defined by the incubator due to the fact that oxygen has to diffuse through the culture medium before reaching the cells. Such phenomenon is aggravated in 3D scaffold culture systems, in which the diffusion limitations are more pronounced, especially when ECM production increases the tissue construct's density<sup>[49,50]</sup>. Therefore, in this study, the lower sGAG amounts observed in tissue constructs cultured under 2%  $\text{O}_2$  tension might be related with diffusional limitations reached in this condition that were not reached in the 5%  $\text{O}_2$  cultures. In fact, a study performed by Malladi and colleagues reported impaired GAG production by adipose-derived MSC micromass differentiated cultures at 2%  $\text{O}_2$  when compared to normoxia<sup>[51]</sup>. It is extremely difficult to make direct comparisons of hypoxia studies due to

dissimilarities in cell sources, culture conditions, scaffold materials and duration of low-oxygen exposure among the different protocols. Further efforts in developing standardized protocols for hypoxic cultures might lead to a broader consensus on the effects of hypoxia in MSC chondrogenesis. Nevertheless, the majority of research supports the use of low-oxygen culture conditions around 3–5%  $\text{O}_2$  tensions to promote *in vitro* MSC chondrogenesis in CTE scaffolds<sup>[49,52]</sup>.

GAGs are main constituents of cartilage and crucial for the maintenance of the structural organization and mechanical properties of the tissue. Decreased GAG (particularly CS and HA) amounts in cartilage tissue have been associated with ageing and pathologies such as osteoarthritis and rheumatoid arthritis<sup>[36,37,53]</sup>. The GAG amounts in human cartilage tissues have been previously reported as a CS concentration of  $18.4 \pm 1.3 \text{ mg/mL}$  in normal adult cartilage, with values ranging from 2 to 4 mg/mL for HA concentration in the synovial fluid from healthy human knee joints<sup>[36–38,53,54]</sup>. Thus, based on the reported values, we used upper limit values of 2% (20 mg/mL) CS and 0.4% (4 mg/mL) HA (w/v) medium solutions to experimentally assess the effects of GAG supplementation on MSC chondrogenic differentiation in 3D PCL scaffolds.

For both MSC sources, CS and HA supplementation did not cause any significant enhancement or detrimental effects on the equivalent cell numbers present in the PCL scaffolds. These results are in accord with Schwartz *et al.*, who also reported no significant differences in equivalent cell numbers in BMSCs-seeded chitosan sponges cultured under different HA-supplemented chondrogenic medium concentrations<sup>[55]</sup>. In the present work, CS and HA supplementation showed beneficial effects on hBMSC/hSMSC chondrogenic differentiation in PCL scaffolds. After 21 days of chondrogenic differentiation, only the HA-supplemented

group resulted in a significant increase in sGAG amounts in both hBMSC-PCL and hSMSC-PCL constructs. Additionally, in hSMSC-PCL constructs, a significant enhancement in sGAG amounts was also observed at an earlier stage (day 14) for the HA-supplemented group when compared to CS-supplemented group. Based on the average values at the end of the experiment, HA-supplementation of hBMSC-PCL constructs resulted in approximately 1.59- and 1.96- fold increase in sGAG amounts relative to non-supplemented and CS-supplemented conditions, respectively. In hSMSC-PCL constructs, the HA-supplemented group resulted in sGAG amounts 2.02- and 2.39-fold higher than the PCL and PCL-CS groups, respectively. Therefore, our results suggest an improved sGAG production by both MSC sources in PCL scaffolds when cultured under HA-supplementation. In accordance with our results, other studies using HA-supplemented medium to promote MSC chondrogenesis in 3D culture systems reported significantly enhanced sGAG amounts relative to the non-supplemented condition<sup>[55,56]</sup>. The addition of CS to chondrogenic medium has also been shown by Chen et al. to stimulate cartilage ECM accumulation during the chondrogenic differentiation of human umbilical cord blood (UCB)-derived MSCs in collagen scaffolds<sup>[57]</sup>. However, their study used chondroitin sulfate C type, which is different from the chondroitin sulfate A sodium salt employed in our study.

Gene expression analysis of the final hBMSC-PCL and hSMSC-PCL constructs showed that GAG supplementation, particularly with HA, promotes the upregulation of chondrogenic marker genes *COL II* and *ACAN* while downregulating the expression of fibrocartilage marker *COL I*. Additionally, hBMSC-PCL constructs showed significant upregulation of hypertrophic marker *COL X* and osteogenic marker *Runx2*, while the hSMSC-PCL constructs exhibited significant downregulation of *COL X* and upregulation of *Runx2* (only significant for cells in the PCL group). However, for both MSC sources, HA and CS supplementation resulted in a significant decrease in *Runx2* expression when compared to the non-supplemented group. The observed chondrogenic genes expression and reduced expression of osteogenic/hypertrophic markers by hSMSC-PCL constructs when supplemented with GAGs may also be related with the hypothesis that hSMSCs are possibly a more “cartilage-tissue specific” stem cell population and therefore more committed for chondrogenesis than hBMSCs<sup>[9]</sup>. In their undifferentiated state before cell seeding (day 0), hSMSCs showed significant upregulation of chondrogenic markers and downregulation of hypertrophy and osteogenic markers when compared to hBMSCs (Supplementary Figure 2), which is accordance with previously published literature<sup>[58]</sup>. Our results also agree with previous studies reporting that supplementation with HA and CS in MSC-based CTE approaches resulted in enhancement of chondrogenic markers expression and suppression of hypertrophic markers<sup>[56,57]</sup>.

All the final hBMSC-PCL and hSMSC-PCL tissue constructs showed presence of defined cell nuclei and cartilage-like ECM composed of proteoglycans and consequently

GAGs. Immunohistological analysis suggests collagen II protein expression with similar intensity among all the constructs but a more intense staining for aggrecan in the constructs cultured with GAG-supplemented medium compared to non-supplemented group, regardless of MSC source. Such observation was in agreement with a previous study highlighting the beneficial effect of HA supplementation in aggrecan deposition by BMSCs<sup>[55]</sup>. TEM analysis revealed the presence of cells embedded in ECM in all experimental groups. Importantly, the presence of collagen fibers characteristic of cartilage ECM was more clearly observed in the hBMSC-PCL and hSMSC-PCL constructs obtained after culture with CS and HA supplemented chondrogenic medium. Moreover, the cell/ECM structures obtained in our analysis were consistent with a previous study reporting TEM analysis of ECM secreted by hBMSCs differentiated in alginate beads after 21 days in chondrogenic medium<sup>[59]</sup>.

In this study, we hypothesized that GAG supplementation could result in improved MSC chondrogenesis through a closer mimicry of the native tissue biochemistry and ECM-cell signaling. However, the addition of GAGs to the culture medium, mainly of high MW HA used in this work, can also result in a closer resemble of synovial fluid viscosity and possibly, in the recapitulation at some extent of the native tissue mechanical cues that can influence differentiation. In fact, Wu et al. demonstrated the benefits of using HA supplementation to simulate synovial fluid properties in the preservation of chondrocyte phenotype when cultured in porous polyurethane scaffolds under mechanical stimulation<sup>[60]</sup>. Therefore, we believe this closer mimicking of the native tissue synovial fluid properties might also played a role in enhancing MSC chondrogenesis in PCL scaffolds, especially in the case of hSMSC.

## 5. Conclusions

In summary, custom-made 3D porous PCL scaffolds were produced and used as platform to study the effects of CS and HA supplementation in the chondrogenic differentiation of hBMSC and hSMSC under hypoxic conditions. GAG supplementation did not promote any significant effect on cell equivalent numbers present in the scaffolds. All experimental groups stained positively for secreted sGAGs, however, for both MSC sources, significantly increased sGAG amounts were only obtained when constructs were cultured with HA-supplemented medium. RT-qPCR analysis showed the upregulation of *COL II* and *ACAN* marker genes, suggesting that GAG supplementation (particularly with HA) supported the hBMSCs and hSMSCs chondrogenic differentiation in PCL scaffolds, however differences between the two MSC sources were observed. All hBMSC-PCL constructs presented upregulation of *COL X*, indicating some degree of tissue hypertrophy, which was not observed for the tissue constructs generated with hSMSCs. Histological, immunohistochemical and TEM analysis confirmed the presence of cartilage-like ECM in all the experimental groups. Nevertheless, future studies should include testing the

*in vivo* performance of the tissue constructs produced under the different experimental conditions to assess the full potential of this integrated CTE strategy. Overall, this study highlights the use of GAG supplementation combined with hSMSCs and customizable 3D scaffolds as a promising strategy to promote MSC chondrogenic differentiation toward the fabrication of improved bioengineered cartilage tissue substitutes.

## Acknowledgements

The authors acknowledge Pedro Henriques for the help with sample preparation for TEM analysis.

## Disclosure statement

The authors confirm that there are no conflicts of interest.

## Funding

The authors acknowledge financial support from Fundação para a Ciência e Tecnologia (FCT, Portugal) through iBB – Institute for Bioengineering and Biosciences [UID/BIO/04565/2019] and from Programa Operacional Regional de Lisboa 2020 [Project N. 007317] and also through the projects PRECISE – Accelerating progress toward the new era of precision medicine [PAC-PRECISE-LISBOA-01-0145-FEDER – 016394], Stimuli2BioScaffold [FCT grant PTDC/EME-SIS/32554/2017]. João C. Silva is grateful to FCT for financial support through the scholarship [SFRH/BD/105771/2014].

## References

- [1] Chen, D.; Shen, J.; Zhao, W.; Wang, T.; Han, L.; Hamilton, J. L.; Im, H.-J. Osteoarthritis: Toward a Comprehensive Understanding of Pathological Mechanism. *Bone Res.* **2017**, *5*, 16044. DOI: [10.1038/boneres.2016.44](https://doi.org/10.1038/boneres.2016.44).
- [2] Tan, A. R.; Hung, C. T. Concise Review: Mesenchymal Stem Cells for Functional Cartilage Tissue Engineering: Taking Cues from Chondrocyte-Based Constructs. *Stem Cells Transl. Med.* **2017**, *6*, 1295–1303. DOI: [10.1002/sctm.16-0271](https://doi.org/10.1002/sctm.16-0271).
- [3] Chamberlain, G.; Fox, J.; Ashton, B.; Middleton, J. Concise Review: Mesenchymal Stem Cells: Their Phenotype, Differentiation Capacity, Immunological Features, and Potential for Homing. *Stem Cells* **2007**, *25*, 2739–2749. DOI: [10.1634/stemcells.2007-0197](https://doi.org/10.1634/stemcells.2007-0197).
- [4] Koga, H.; Muneta, T.; Nagase, T.; Nimura, A.; Ju, Y. J.; Mochizuki, T.; Sekiya, I. Comparison of Mesenchymal Tissue-Derived Stem Cells for *in Vivo* Chondrogenesis: Suitable Conditions for Cell Therapy of Cartilage Defects in Rabbit. *Cell Tissue Res.* **2008**, *333*, 207–215. DOI: [10.1007/s00441-008-0633-5](https://doi.org/10.1007/s00441-008-0633-5).
- [5] Sakaguchi, Y.; Sekiya, I.; Yagishita, K.; Muneta, T. Comparison of Human Stem Cells Derived from Various Mesenchymal Tissues: Superiority of Synovium as a Cell Source. *Arthritis Rheum.* **2005**, *52*, 2521–2529. DOI: [10.1002/art.21212](https://doi.org/10.1002/art.21212).
- [6] Yoshimura, H.; Muneta, T.; Nimura, A.; Yokoyama, A.; Koga, H.; Sekiya, I. Comparison of Rat Mesenchymal Stem Cells Derived from Bone Marrow, Synovium, Periosteum, Adipose Tissue, and Muscle. *Cell Tissue Res.* **2007**, *327*, 449–462. DOI: [10.1007/s00441-006-0308-z](https://doi.org/10.1007/s00441-006-0308-z).
- [7] Huang, Y.-Z.; Silini, A.; Parolini, O.; Xie, H.-Q.; Huang, Y.-C.; Zhang, Y.; Deng, L. Mesenchymal Stem/Progenitor Cells Derived from Articular Cartilage, Synovial Membrane and Synovial Fluid for Cartilage Regeneration: Current Status and Future Perspectives. *Stem Cell Rev. Rep.* **2017**, *13*, 575–586. DOI: [10.1007/s12015-017-9753-1](https://doi.org/10.1007/s12015-017-9753-1).
- [8] Futami, I.; Ishijima, M.; Kaneko, H.; Tsuji, K.; Ichikawa-Tomikawa, N.; Sadatsuki, R.; Muneta, T.; Arikawa-Hirasawa, E.; Sekiya, I.; Kaneko, K. Isolation and Characterization of Multipotential Mesenchymal Cells from the Mouse Synovium. *PLoS One* **2012**, *7*, e45517. DOI: [10.1371/journal.pone.0045517](https://doi.org/10.1371/journal.pone.0045517).
- [9] Fan, J.; Varshney, R. R.; Ren, L.; Cai, D.; Wang, D. A. Synovium-Derived Mesenchymal Stem Cells: A New Cell Source for Musculoskeletal Regeneration. *Tissue Eng. B. Rev.* **2009**, *15*, 75–86. DOI: [10.1089/ten.teb.2008.0586](https://doi.org/10.1089/ten.teb.2008.0586).
- [10] Shirasawa, S.; Sekiya, I.; Sakaguchi, Y.; Yagishita, K.; Ichinose, S.; Muneta, T. *In Vitro* Chondrogenesis of Human Synovium-Derived Mesenchymal Stem Cells: Optimal Condition and Comparison with Bone Marrow-Derived Cells. *J. Cell. Biochem.* **2006**, *97*, 84–97. DOI: [10.1002/jcb.20546](https://doi.org/10.1002/jcb.20546).
- [11] Mota, C.; Puppi, D.; Chiellini, F.; Chiellini, E. Additive Manufacturing Techniques for the Production of Tissue Engineering Constructs. *J. Tissue Eng. Regen. Med.* **2015**, *9*, 174–190. DOI: [10.1002/term.1635](https://doi.org/10.1002/term.1635).
- [12] Hoque, M. E.; Chuan, Y. L.; Pashby, I. Extrusion Based Rapid Prototyping Technique: An Advanced Platform for Tissue Engineering Scaffold Fabrication. *Biopolymers* **2012**, *97*, 83–93. DOI: [10.1002/bip.21701](https://doi.org/10.1002/bip.21701).
- [13] Woodruff, M. A.; Huttmacher, D. W. The Return of a Forgotten Polymer - Polycaprolactone in the 21st Century. *Prog. Polym. Sci.* **2010**, *35*, 1217–1256. DOI: [10.1016/j.progpolymsci.2010.04.002](https://doi.org/10.1016/j.progpolymsci.2010.04.002).
- [14] Theodoridis, K.; Aggelidou, E.; Vavilis, T.; Manthou, M. E.; Tsimponis, A.; Demiri, E. C.; Boukla, A.; Salpistis, C.; Bakopoulou, A.; Mihailidis, A.; Kritis, A. Hyaline Cartilage Next Generation Implants from Adipose Tissue Derived Mesenchymal Stem Cells: Comparative Study on 3D-Printed Polycaprolactone Scaffold Patterns. *J. Tissue Eng. Regen. Med.* **2019**, *13*, 342–355. DOI: [10.1002/term.2798](https://doi.org/10.1002/term.2798).
- [15] Kim, H. J.; Lee, J. H.; Il Im, G. Chondrogenesis Using Mesenchymal Stem Cells and PCL Scaffolds. *J. Biomed. Mater. Res.* **2010**, *92*, 659–666. DOI: [10.1002/jbm.a.32414](https://doi.org/10.1002/jbm.a.32414).
- [16] Vinatier, C.; Mrugala, D.; Jorgensen, C.; Guicheux, J.; Noël, G. Cartilage Engineering: A Crucial Combination of Cells, Biomaterials and Biofactors. *Trends Biotechnol.* **2009**, *27*, 307–314. DOI: [10.1016/j.tibtech.2009.02.005](https://doi.org/10.1016/j.tibtech.2009.02.005).
- [17] Pattappa, G.; Johnstone, B.; Zellner, J.; Docheva, D.; Angele, P. The Importance of Physioxia in Mesenchymal Stem Cell Chondrogenesis and the Mechanisms Controlling Its Response. *Int. J. Mol. Sci.* **2019**, *20*, 1–28. DOI: [10.3390/ijms20030484](https://doi.org/10.3390/ijms20030484).
- [18] Zhou, S.; Cui, Z.; Urban, J. P. G. Factors Influencing the Oxygen Concentration Gradient from the Synovial Surface of Articular Cartilage to the Cartilage-Bone Interface: A Modeling Study. *Arthritis Rheum.* **2004**, *50*, 3915–3924. DOI: [10.1002/art.20675](https://doi.org/10.1002/art.20675).
- [19] Lund-Olesen, K. Oxygen Tension in Synovial Fluids. *Arthritis Rheum.* **1970**, *13*, 769–776. DOI: [10.1002/art.1780130606](https://doi.org/10.1002/art.1780130606).
- [20] Ferro, T.; Santhaganam, A.; Madeira, C.; Salgueiro, J. B.; da Silva, C. L.; Cabral, J. M. S. Successful Isolation and *Ex Vivo* Expansion of Human Mesenchymal Stem/Stromal Cells Obtained from Different Synovial Tissue-Derived (Biopsy) Samples. *J. Cell. Physiol.* **2019**, *234*, 3973–3984. DOI: [10.1002/jcp.27202](https://doi.org/10.1002/jcp.27202).
- [21] Dos Santos, F.; Andrade, P. Z.; Boura, J. S.; Abecasis, M. M.; da Silva, C. L.; Cabral, J. M. S. *Ex Vivo* Expansion of Human Mesenchymal Stem Cells: A More Effective Cell Proliferation Kinetics and Metabolism under Hypoxia. *J. Cell. Physiol.* **2010**, *223*, 27–35. DOI: [10.1002/jcp.21987](https://doi.org/10.1002/jcp.21987).
- [22] Adesida, A. B.; Mulet-Sierra, A.; Jomha, N. M. Hypoxia Mediated Isolation and Expansion Enhances the Chondrogenic Capacity of Bone Marrow Mesenchymal Stromal Cells. *Stem Cell Res. Ther.* **2012**, *3*, 9. DOI: [10.1186/scrt10022385573](https://doi.org/10.1186/scrt10022385573).
- [23] Leijten, J.; Georgi, N.; Moreira Teixeira, L.; van Blitterswijk, C. A.; Post, J. N.; Karperien, M. Metabolic Programming of



- Mesenchymal Stromal Cells by Oxygen Tension Directs Chondrogenic Cell Fate. *Proc. Natl. Acad. Sci.* **2014**, *111*, 13954–13959. DOI: [10.1073/pnas.1410977111](https://doi.org/10.1073/pnas.1410977111).
- [24] Bae, H. C.; Park, H. J.; Wang, S. Y.; Yang, H. R.; Lee, M. C.; Han, H.-S. Hypoxic Condition Enhances Chondrogenesis in Synovium-Derived Mesenchymal Stem Cells. *Biomater. Res.* **2018**, *22*, 1–8. DOI: [10.1186/s40824-018-0134-x](https://doi.org/10.1186/s40824-018-0134-x).
- [25] Bornes, T. D.; Jomha, N. M.; Mulet-Sierra, A.; Adesida, A. B. Hypoxic Culture of Bone Marrow-Derived Mesenchymal Stromal Stem Cells Differentially Enhances in Vitro Chondrogenesis within Cell-Seeded Collagen and Hyaluronic Acid Porous Scaffolds. *Stem Cell Res Ther.* **2015**, *6*, 84. DOI: [10.1186/s13287-015-0075-4](https://doi.org/10.1186/s13287-015-0075-4).
- [26] Gasimli, L.; Linhardt, R. J.; Dordick, J. S. Proteoglycans in Stem Cells. *Biotechnol. Appl. Biochem.* **2012**, *59*, 65–76. DOI: [10.1002/bab.1002](https://doi.org/10.1002/bab.1002).
- [27] Knudson, C. B.; Knudson, W. Cartilage Proteoglycans. *Semin. Cell Dev. Biol.* **2001**, *12*, 69–78. DOI: [10.1007/978-3-319-29568-8\\_1](https://doi.org/10.1007/978-3-319-29568-8_1).
- [28] Oliveira, J. T.; Reis, R. L. Polysaccharide-Based Materials for Cartilage Tissue Engineering Applications. *J. Tissue Eng. Regen. Med.* **2011**, *5*, 421–436. DOI: [10.1002/term.335](https://doi.org/10.1002/term.335).
- [29] Wang, M.; Liu, X.; Lyu, Z.; Gu, H.; Li, D.; Chen, H. Glycosaminoglycans (GAGs) and GAG Mimetics Regulate the Behavior of Stem Cell Differentiation. *Colloids Surf. B Biointerfaces* **2017**, *150*, 175–182. DOI: [10.1016/j.colsurfb.2016.11.022](https://doi.org/10.1016/j.colsurfb.2016.11.022).
- [30] Sawatjui, N.; Damrongrungruang, T.; Leeanansaksiri, W.; Jearanaikoon, P.; Hongeng, S.; Limpai boon, T. Silk Fibroin/Gelatin-Chondroitin Sulfate-Hyaluronic Acid Effectively Enhances in Vitro Chondrogenesis of Bone Marrow Mesenchymal Stem Cells. *Mater. Sci. Eng. C* **2015**, *52*, 90–96. DOI: [10.1016/j.msec.2015.03.043](https://doi.org/10.1016/j.msec.2015.03.043).
- [31] Varghese, S.; Hwang, N. S.; Canver, A. C.; Theprungsirikul, P.; Lin, D. W.; Elisseff, J. Chondroitin Sulfate Based Niches for Chondrogenic Differentiation of Mesenchymal Stem Cells. *Matrix Biol.* **2008**, *27*, 12–21. DOI: [10.1016/j.matbio.2007.07.002](https://doi.org/10.1016/j.matbio.2007.07.002).
- [32] Pfeifer, C. G.; Berner, A.; Koch, M.; Krutsch, W.; Kujat, R.; Angele, P.; Nerlich, M.; Zellner, J. Higher Ratios of Hyaluronic Acid Enhance Chondrogenic Differentiation of Human MSCs in a Hyaluronic Acid-Gelatin Composite Scaffold. *Materials* **2016**, *9*, 381. DOI: [10.3390/ma9050381](https://doi.org/10.3390/ma9050381).
- [33] Santhagunam, A.; Dos Santos, F.; Madeira, C.; Salgueiro, J. B.; Cabral, J. M. S. Isolation and Ex Vivo Expansion of Synovial Mesenchymal Stromal Cells for Cartilage Repair. *Cytotherapy* **2014**, *16*, 440–453. DOI: [10.1016/j.jcyt.2013.10.010](https://doi.org/10.1016/j.jcyt.2013.10.010).
- [34] Domingos, M.; Dinucci, D.; Cometa, S.; Alderighi, M.; Bártolo, P. J.; Chiellini, F. Polycaprolactone Scaffolds Fabricated via Bioextrusion for Tissue Engineering Applications. *Int. J. Biomater.* **2009**, *2009*, 239643. DOI: [10.1155/2009/239643](https://doi.org/10.1155/2009/239643).
- [35] Silva, J. C.; Moura, C. S.; Alves, N.; Cabral, J. M. S.; Ferreira, F. C. Effects of Different Fibre Alignments and Bioactive Coatings on Mesenchymal Stem/Stromal Cell Adhesion and Proliferation in Poly (ε-Caprolactone) Scaffolds towards Cartilage Repair. *Procedia Manuf.* **2017**, *12*, 132–140. DOI: [10.1016/j.promfg.2017.08.034](https://doi.org/10.1016/j.promfg.2017.08.034).
- [36] Bollet, A. J.; Nance, J. L. Biochemical Findings in Normal and Osteoarthritic Articular Cartilage. II. Chondroitin Sulfate Concentration and Chain Length, Water, and Ash Content. *J. Clin. Invest.* **1966**, *45*, 1170–1177. DOI: [10.1172/JCI105423](https://doi.org/10.1172/JCI105423).
- [37] Nakayama, Y.; Narita, T.; Mori, A.; Uesaka, S.; Miyazaki, K.; Ito, H. The Effects of Age and Sex on Chondroitin Sulfates in Normal Synovial Fluid. *Arthritis Rheum.* **2002**, *46*, 2105–2108. DOI: [10.1002/art.10424](https://doi.org/10.1002/art.10424).
- [38] Mazzucco, D.; Scott, R.; Spector, M. Composition of Joint Fluid in Patients Undergoing Total Knee Replacement and Revision Arthroplasty: Correlation with Flow Properties. *Biomaterials* **2004**, *25*, 4433–4445. DOI: [10.1016/j.biomaterials.2003.11.023](https://doi.org/10.1016/j.biomaterials.2003.11.023).
- [39] Dingle, J. T.; Horsfield, P.; Fell, H. B.; Barratt, M. E. J. Breakdown of Proteoglycan and Collagen Induced in Pig Articular Cartilage in Organ Culture. *Ann. Rheum. Dis.* **1975**, *34*, 303–311. DOI: [10.1136/ard.34.4.303](https://doi.org/10.1136/ard.34.4.303).
- [40] Nam, J.; Johnson, J.; Lannutti, J. J.; Agarwal, S. Modulation of Embryonic Mesenchymal Progenitor Cell Differentiation via Control over Pure Mechanical Modulus in Electrospun Nanofibers. *Acta Biomater.* **2011**, *7*, 1516–1524. DOI: [10.1016/j.actbio.2010.11.022](https://doi.org/10.1016/j.actbio.2010.11.022).
- [41] Olubamiji, A. D.; Izadifar, Z.; Si, J. L.; Cooper, D. M. L.; Eames, B. F.; Chen, D. X. B. Modulating Mechanical Behaviour of 3D-Printed Cartilage-Mimetic PCL Scaffolds: Influence of Molecular Weight and Pore Geometry. *Biofabrication* **2016**, *8*, 025020. DOI: [10.1088/1758-5090/8/2/025020](https://doi.org/10.1088/1758-5090/8/2/025020).
- [42] Zhao, Y.; Tan, K.; Zhou, Y.; Ye, Z.; Tan, W. S. A Combinatorial Variation in Surface Chemistry and Pore Size of Three-Dimensional Porous Poly(ε-Caprolactone) Scaffolds Modulates the Behaviors of Mesenchymal Stem Cells. *Mater. Sci. Eng. C* **2016**, *59*, 193–202. DOI: [10.1016/j.msec.2015.10.017](https://doi.org/10.1016/j.msec.2015.10.017).
- [43] Im, G. I.; Ko, J. Y.; Lee, J. H. Chondrogenesis of Adipose Stem Cells in a Porous Polymer Scaffold: Influence of the Pore Size. *Cell Transplant.* **2012**, *21*, 2397–2405. DOI: [10.3727/096368912X638865](https://doi.org/10.3727/096368912X638865).
- [44] Jeon, O.; Alsberg, E. Regulation of Stem Cell Fate in a Three-Dimensional Micropatterned Dual-Crosslinked Hydrogel System. *Adv. Funct. Mater.* **2013**, *23*, 4764–4775. DOI: [10.1002/adfm.201300529](https://doi.org/10.1002/adfm.201300529).
- [45] Nieto, A.; Dua, R.; Zhang, C.; Boesl, B.; Ramaswamy, S.; Agarwal, A. Three Dimensional Graphene Foam/Polymer Hybrid as a High Strength Biocompatible Scaffold. *Adv. Funct. Mater.* **2015**, *25*, 3916–3924. DOI: [10.1002/adfm.201500876](https://doi.org/10.1002/adfm.201500876).
- [46] Grayson, W. L.; Zhao, F.; Izadpanah, R.; Bunnell, B.; Ma, T. Effects of Hypoxia on Human Mesenchymal Stem Cell Expansion and Plasticity in 3D Constructs. *J. Cell. Physiol.* **2006**, *207*, 331–339. DOI: [10.1002/jcp.20571](https://doi.org/10.1002/jcp.20571).
- [47] Huang, X.; Hou, Y.; Zhong, L.; Huang, D.; Qian, H.; Karperien, M.; Chen, W. Promoted Chondrogenesis of Cocultured Chondrocytes and Mesenchymal Stem Cells under Hypoxia Using in-Situ Forming Degradable Hydrogel Scaffolds. *Biomacromolecules* **2018**, *19*, 94–102. DOI: [10.1021/acs.biomac.7b01271](https://doi.org/10.1021/acs.biomac.7b01271).
- [48] Rodenas-Rochina, J.; Kelly, D. J.; Gómez Ribelles, J. L.; Lebourg, M. Influence of Oxygen Levels on Chondrogenesis of Porcine Mesenchymal Stem Cells Cultured in Polycaprolactone Scaffolds. *J. Biomed. Mater. Res. A* **2017**, *105*, 1684–1691. DOI: [10.1002/jbm.a.36043](https://doi.org/10.1002/jbm.a.36043).
- [49] Das, R.; Jahr, H.; Van Osch, G. J. V. M.; Farrell, E. The Role of Hypoxia in Bone Marrow – Derived Mesenchymal Stem Cells: Considerations for Regenerative Medicine Approaches. *Tissue Eng. B. Rev* **2010**, *16*, 159–168. DOI: [10.1089/ten.teb.2009.0296](https://doi.org/10.1089/ten.teb.2009.0296).
- [50] Fink, T.; Abildtrup, L.; Fogd, K.; Abdallah, B. M.; Kassem, M.; Ebbesen, P.; Zachar, V. Induction of Adipocyte-Like Phenotype in Human Mesenchymal Stem Cells by Hypoxia. *Stem Cells* **2004**, *22*, 1346–1355. DOI: [10.1634/stemcells.2004-0038](https://doi.org/10.1634/stemcells.2004-0038).
- [51] Malladi, P.; Xu, Y.; Chiou, M.; Giaccia, A. J.; Longaker, M. T. Effect of Reduced Oxygen Tension on Chondrogenesis and Osteogenesis in Adipose-Derived Mesenchymal Cells. *Am. J. Physiol. Cell Physiol* **2006**, *290*, 1139–1146. DOI: [10.1152/ajp-cell.00415.2005](https://doi.org/10.1152/ajp-cell.00415.2005).
- [52] Gaut, C.; Sugaya, K. Critical Review on the Physical and Mechanical Factors Involved in Tissue Engineering of Cartilage. *Regen. Med.* **2015**, *10*, 665–679. DOI: [10.2217/rme.15.31](https://doi.org/10.2217/rme.15.31).
- [53] Temple-Wong, M. M.; Ren, S.; Quach, P.; Hansen, B. C.; Chen, A. C.; Hasegawa, A.; D’Lima, D. D.; Koziol, J.; Masuda, K.; Lotz, M. K.; Sah, R. L. Hyaluronan Concentration and Size Distribution in Human Knee Synovial Fluid: Variations with Age and Cartilage degeneration. *Arthritis Res. Ther.* **2016**, *18*, 18. DOI: [10.1186/s13075-016-0922-4](https://doi.org/10.1186/s13075-016-0922-4).
- [54] Balazs, E. A. The Physical Properties of Synovial Fluid and the Special Role of Hyaluronic Acid. *Disord. Knee* **1974**, *2*, 61–74.
- [55] Schwartz, Z.; Griffon, D. J.; Fredericks, L. P.; Lee, H.-B.; Weng, H.-Y. Hyaluronic Acid and Chondrogenesis of Murine Bone



- Marrow Mesenchymal Stem Cells in Chitosan Sponges. *Am. J. Vet. Res.* **2011**, *72*, 42–50. DOI: [10.2460/ajvr.72.1.42](https://doi.org/10.2460/ajvr.72.1.42).
- [56] Christiansen-Weber, T.; Noskov, A.; Cardiff, D.; Garitaonandia, I.; Dillberger, A.; Semechkin, A.; Gonzalez, R.; Kern, R. Supplementation of Specific Carbohydrates Results in Enhanced Deposition of Chondrogenic-Specific Matrix during Mesenchymal Stem Cell Differentiation. *J. Tissue Eng. Regen. Med.* **2018**, *12*, 1261–1272. DOI: [10.1002/term.2658](https://doi.org/10.1002/term.2658).
- [57] Chen, W. C.; Yao, C. L.; Chu, I. M.; Wei, Y. H. Compare the Effects of Chondrogenesis by Culture of Human Mesenchymal Stem Cells with Various Type of the Chondroitin Sulfate C. *J. Biosci. Bioeng.* **2011**, *111*, 226–231. DOI: [10.1016/j.jbiosec.2010.10.002](https://doi.org/10.1016/j.jbiosec.2010.10.002).
- [58] Ogata, Y.; Mabuchi, Y.; Yoshida, M.; Suto, E. G.; Suzuki, N.; Muneta, T.; Sekiya, I.; Akazawa, C. Purified Human Synovium Mesenchymal Stem Cells as a Good Resource for Cartilage Regeneration. *PLoS One* **2015**, *10*, e0129096. DOI: [10.1371/journal.pone.0129096](https://doi.org/10.1371/journal.pone.0129096).
- [59] Dashtdar, H.; Murali, M. R.; Selvaratnam, L.; Balaji Raghavendran, H.; Suhaeb, A. M.; Ahmad, T. S.; Kamarul, T. Ultra-Structural Changes and Expression of Chondrogenic and Hypertrophic Genes during Chondrogenic Differentiation of Mesenchymal Stromal Cells in Alginate Beads. *PeerJ* **2016**, *4*, e1650. DOI: [10.7717/peerj.1650](https://doi.org/10.7717/peerj.1650).
- [60] Wu, Y.; Stoddart, M. J.; Wuertz-Kozak, K.; Grad, S.; Alini, M.; Ferguson, S. J. Hyaluronan Supplementation as a Mechanical Regulator of Cartilage Tissue Development under Joint-Kinematic Mimicking Loading. *J. R. Soc. Interface* **2017**, *14*, 20170255. DOI: [10.1098/rsif.2017.0255](https://doi.org/10.1098/rsif.2017.0255).